Internal Report ITESRE 197/1997

NEW DESIGN OF PLANCK TELESCOPE

F.Villa[1], M.Bersanelli[2], N.Mandolesi[1],
L.Valenziano[1]

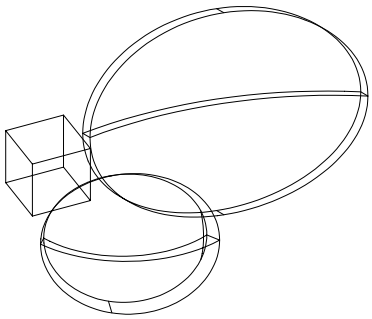

[1]*Istituto TESRE, CNR, Bologna, Italy*
[2]*Istituto di Fisica Cosmica, CNR, Milano, Italy*

October 1997

Internal Report ITESRE 197/1997

NEW DESIGN OF PLANCK TELESCOPE

F.Villa[1], M.Bersanelli[2], N.Mandolesi[1], L.Valenziano[1]

[1]*Istituto TESRE, CNR, Bologna, Italy*
[2]*Istituto di Fisica Cosmica, CNR, Milano, Italy*

SUMMARY —- The recent rearrangement of the payload of the FIRST / PLANCK mission has required a new design of the LFI telescope. Considering the scientific objectives of the PLANCK experiment, the goal of this study is to propose a telescope with a main reflector larger than in the previous design. Starting from COBRAS/SAMBA configuration, presented in COBRAS/SAMBA *report on the phase A study* and, in detail, in TICRA *report S-699-02*, we propose a *New Gregorian Off-Axis Telescope*, enlarged to fill the available room inside the cylindrical shield of LFI payload section. We present in this report the optical project, based on geometrical optic design (section 2), and some electrical calculation carried out at 30GHz and 100GHz (section 3). Several considerations on simulation results and geometrical constraints are reported in section 4.

1 Introduction

The high sensivity required by the measurements of the anisotropies of the Cosmic Microwave Background Radiation needs a specific telescope design. In particular, the necessity to have a very low level of side lobes, low level of cross-polarization and a complex focal plane, requires an offset Gregorian reflector system. This configuration is arranged by a parabolic main reflector and an ellipsoid as secondary reflector. The offset configuration is studied in order to obtain a telescope free of blockage in the aperture plane, for small scan angles also. The location of the axis of symmetry of each reflector is chosen to reduce the cross polarization.

sectionDesign of new configurations

Optical parameters of the "*original*" COBRAS/SAMBA telescope configuration, called Conf.#0, are reported in table 1, column 1.

It is readily seen in figure 2, upper table, that the optical design of the telescope does not exploit all the room available inside the LFI outer shield. This consideration suggests that an enlarged telescope can be allocated in this place.

New configurations are developed from simple geometrical optic calculations. Once the basic parameters have been defined, a simple code can be implemented to calculate all the other design parameters from which external size of the telescope can be obtained.

In the basic "*enlarged* " configuration, Conf.#1, diameter of the primary mirror and major axis of the secondary mirror have been increased, maintaining the same subreflector eccentricity, the same focal ratio and the same offset angle. Conf.#1 parameters are presented in table 1. The schematic design, with main dimensions, is presented in the upper table of Figure 3.

A completely new configuration, Conf.#2, has been conceived to reduce spillover effects at the top edge of the primary mirror. The design of this configuration is displayed in the bottom draw of the Figure 3.

This configuration have the same subreflector of Conf.#0. The parabola that generates main reflector surface is the same of the *original* telescope, but main reflector rim is oversized. Thus, the central ray coming from the subreflector is not pointed anymore towards the center of primary reflector aperture, as it is in Conf.#0 and Conf.#1. This is an important difference between Conf.#2 and both Conf.#0 (*original*) and Conf.#1 (*enlarged*).

2 Electrical characteristics

Up till now, only main reflector radiating performances has been analyzed, modelling the PLANCK telescope as an off-axis single reflector telescope for each configuration.

The subreflector scattered field has been modelled with a symmetrical beam feed with a taper of -3dB at 15^o (called *"primary beam"*). This is similar to the beam outcoming from subreflector in the symmetry plane, but is also symmetric in the telescope asymmetry plane.

The analysis was carried out in two subsequent steps. In the first one, the *primary beam* pointing direction was selected by satisfying the *Dragone-Mizuguchi* condition for Conf.#1 design. The same direction was used to evaluate Conf.#2 performances. The main characteristic of this choice is that angles θ_a and θ_b in figure 2 are not equal, producing different tapers at the bottom and top edges of the primary reflector. Results are presented in Figure 4 (telescope symmetry plane) and in Figure 5 (telescope asymmetry plane).

The second step was implemented to obtain equal tapers at both edges of Conf.#1 primary reflector. This leads to a better modelling of far lobe effects. Indeed, the real subreflector scattered field is asymmetric in the telescope asymmetric plane, and it produces similar tapers at main reflector edges. To include this effect in our modelling, the pointing direction of the *primary beam* (which is symmetric) has to be modified.

Equal tapers at Conf.#1 reflector edges are obtained by choosing $\theta_a = \theta_b$ in Figure 2.

Conf.#2 has been developed to obtain a lower far lobes level, by extending the top edge of the primary reflector. To compare Conf.#2 to the two other configurations, the *primary beam* pointing direction is required to be the same. Obviously, $\theta_a \neq \theta_b$ in this case and thus, tapers are different.

Results are presented in Figure 6 and Figure 7.

The analysis has been computed with GTD (Geometrical Theory of Diffraction) for far lobes and PO (Physical Optics) for radiation near main beam, in order to evaluated directivity and HPBW.

In the following subsections we report the results of the analysis of side lobes level and directivity. Cross-polar characteristics of these new configuration have not been analyzed yet, because they depend strongly on the subreflector scattered field.

2.1 Side Lobes Level

Figures 4,5,6 and 7 show the predicted Far-Field performances of the two new optical configurations presented in this report, compared to the Far-Field performances of *Original* telescope.

Each telescope configuration has been analyzed with *asymmetric* ($\Theta_a \neq \Theta_b$ in Conf.#1) and *symmetric* ($\Theta_a = \Theta_b$ in Conf.#1) subreflector scattered field.

It is evident, by comparing Conf.#0 in figure 4 and Conf.#0 in figure 6, that the *symmetric* model better represents the real subreflector illumination. The two different *primary beam* pointing directions generate different side lobes level for each of the three configurations.

As expected, diffraction effects due to the top edge of the main reflector are reduced in Conf.#2, as it is readily seen in both figure 4 and figure 6.

Conf.#1 have the same side lobe level of the Conf.#0 because it is obtained by scaling the *original* telescope. Thus, illumination is almost equal for these two configurations.

2.2 Directivity and HPBW

Results of calculations at 30 GHz and 100 GHz are reported in table 2 and table 3. Conf.#1 provide a substantially increment of the directivity and a reduction of the HPBW, due to the larger main reflector diameter. In Conf.#2 the larger diameter of primary mirror provides a lower reduction of HPBW than in Conf.#1, because the main reflector is under illuminated by the *primary beam*.

3 Conclusions

Analysis of two new configurations has been carried out in order to propose a new optical design of Planck-LFI telescope.

Both configurations reported have a primary mirror larger than the main reflector of Phase A telescope configuration (Conf.#0).

The focal plane illumination of the *original* telescope has been retained in all the configurations considered here.

Conf.#1 has been studied in order to get a HPBW lower than one of Conf.#0. The side lobes level, in both configurations, is substantially unchanged ($\sim -50dB$ respect to the maximum).

Conf.#2 is proposed to provide a little increment of directivity but a great reduction of the level of the top edge side lobe ($\sim -70dB$ respect to the maximum) compared to Conf.#0 and Conf.#1.

4 Appendix: Geometrical Considerations

We report here some interesting geometrical formulae for a gregorian off-axis telescope. Geometrical parameters have been defined in a reference coordinate system displayed in figure 1. The origin of the coordinate system is chosen at the vertex of the parabola and the Z-axis coincides with the parabola axis of revolution.

The starting point for the telescope design is the *Dragone-Mizuguchi* condition:

$$\tan\alpha = M \cdot \tan\beta \tag{1}$$

where 2β is the offset angle between the parabola axis and the ellipse axis, 2α is the angle between the ellipse axis and the axis of the feedhorn in the focal plane, M is the magnitude of secondary mirror defined by

$$M = \left| \frac{e+1}{e-1} \right| \tag{2}$$

where e is the eccentricity of the ellipse. Under this condition, cross-polarization is suppressed and the off-axis dual reflector system is equivalent to a single on-axis reflector with

$$\begin{aligned} D_{eq} &= D_p \\ F_{eq} &= M \cdot F_p \end{aligned} \tag{3}$$

where D_p and F_p are the projected aperture diameter and the focal length of the primary parabolic mirror of the gregorian telescope.

There are geometrical constraints on the choice of the primary mirror diameter if the direction of the central ray, outcoming from the subreflector, intersects the main reflector at the center of the projected aperture.

We will show that, fixed the offset angle 2β, under the *Dragone-Mizuguchi* condition, the direction of the central ray from subreflector to main reflector depends only on the 2β and magnitude M of subreflector.

It can be seen in figure 1, considering the triangle $F_0V_0F_1$, that

$$\frac{F_1V_0}{2 \cdot c} = \frac{\sin 2\alpha}{\sin 2i} \tag{4}$$

where $2c$ is the focal length of the ellipse. From geometrical properties of ellipse we have that

$$F_1V_0 = \frac{a\left(1-e^2\right)}{1 + e \cdot \cos(2\gamma + 2\beta)} \tag{5}$$

where a is the half major axis of the ellipse.

Substituting the equation (5) in (4), remembering that $e = \frac{c}{a}$, we get

$$\frac{\sin 2\alpha}{\sin 2i} = \frac{a\left(1-e^2\right)}{2e \cdot (1 + e \cdot \cos(2\gamma + 2\beta))} \tag{6}$$

Equation (6) is satisfied for two different values of γ:

Always for

$$\gamma = -\pi/2 \tag{7}$$

and for any γ which satisfy the equation

$$\tan(\gamma + \beta) = M^2 \cdot \tan\beta \tag{8}$$

This last equation, along with equation (1) define the path (from feed to main reflector) of the central ray that minimize the cross-polarization of the offset gregorian telescope [1] and the solution yields an optimal strategy for the telescope design.

The coordinates in the asymmetry plane of the point C, which is the intersection between the central ray direction and the parabolic profile of the main mirror, are

$$x_C = \frac{2F_p}{m} \cdot \left(1 - \sqrt{1+m^2}\right) \tag{9}$$

$$z_C = \frac{1}{4F_p} \cdot x_C^2 \tag{10}$$

[1] this system of equations is readily generalized for Cassegrain systems

where $m = \tan(\pi - 2\gamma)$. If the point C is coincident with the center of the aperture of the main reflector, the parabolic mirror edges, A (low edge) and B (high edge), have coordinates

$$\begin{aligned} x_A &= x_C - \frac{D_p}{2} \\ z_A &= \frac{1}{4F_p} \cdot x_A^2 \end{aligned} \tag{11}$$

$$\begin{aligned} x_B &= x_C + \frac{D_p}{2} \\ z_B &= \frac{1}{4F_p} \cdot x_B^2 \end{aligned} \tag{12}$$

Therefore if the parameters D_p, F_p, M and 2β are fixed, and the condition (1) is satisfied, the main reflector is completely determined by solving equation (8) and then equations (11) and (12).

REFERENCES

1. L.V.Blake, 1966, *Antennas*, Wiley series in Electronic Engineering Technology
2. W.N.Christiansen, J.A.Hogbom, 1969, *Radiotelescopes*, Cambridge at the University Press
3. R.E.Collins, 1985, *Antennas and Radiowave Propagation*, McGraw-Hill International Editions - Electrical Engineering Series
4. C.Dragone, 1978, *The Bell System Technical Journal*, **57**, No. 7, 2663
5. J.D.Kraus, 1950, *Antennas*, McGraw-Hill Book Company - Electrical and Electronic Engineering Series
6. Y.Mizuguchi *et al.* , 1978, *Electronic and Communication in Japan*, **61-B**, No. 3, 58
7. P.H. Nielsen and K. Pontoppidan, 1996, *Design and analysis of the COBRAS/SAMBA telescope*, TICRA report S-699-02
8. W.V.T.Rush, A.Prata, Y.Rahmat-Samii, R.A.Shore, 1990, *IEEE Trans. AP*, **38**, No. 8, 1141-1149
9. VV.AA., 1996, *COBRAS/SAMBA, report on the phase A study*, ESA report D/SCI(96)3
10. B.S.Westcott *et al.* , 1981, *IEE Proceeding*, **181**, Pt.H, No. 1
11. P.J.Wood, *Reflector antenna analysis and design*, IEE electromagnetic series 7

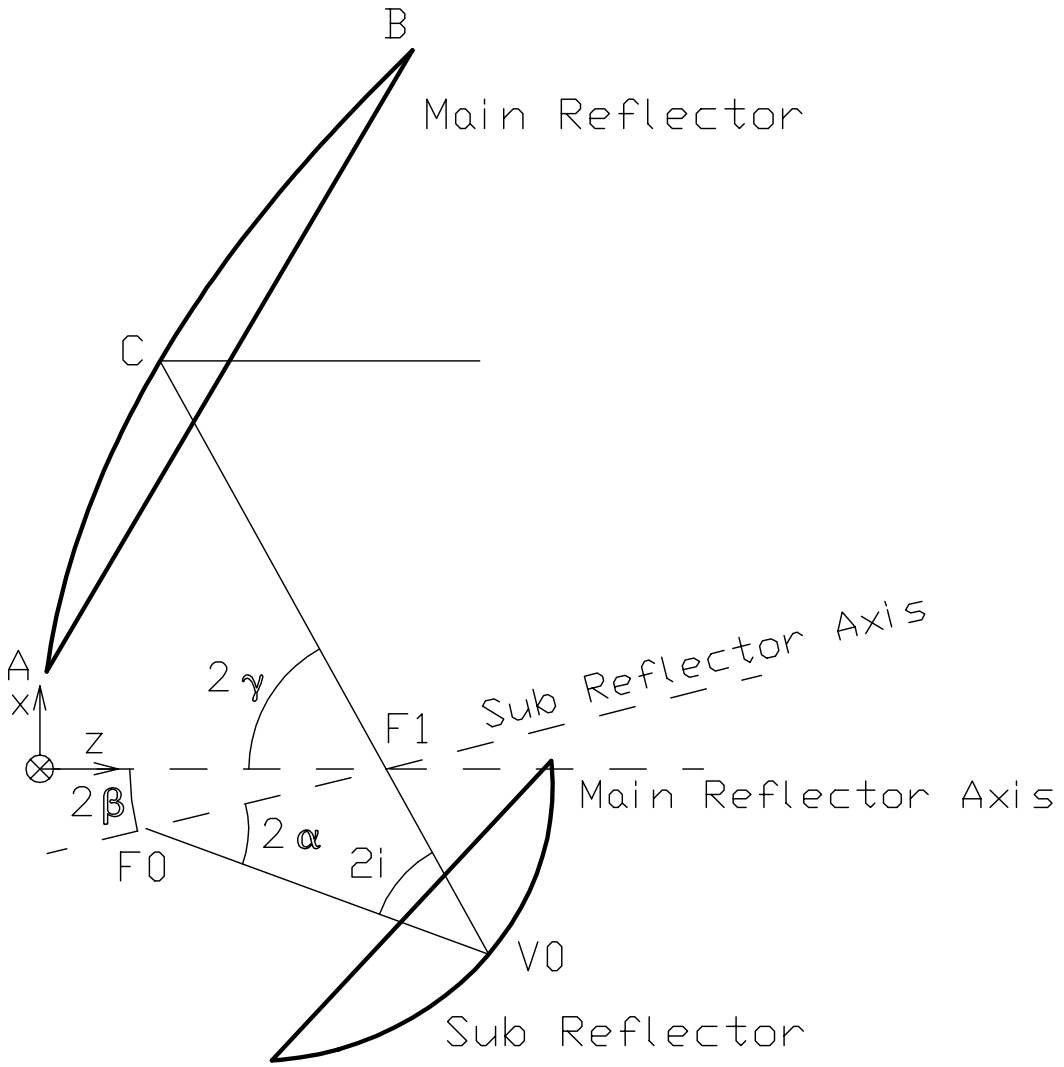

Figure 1: optical setup for a general gregorian off-axis telescope: parameters definition

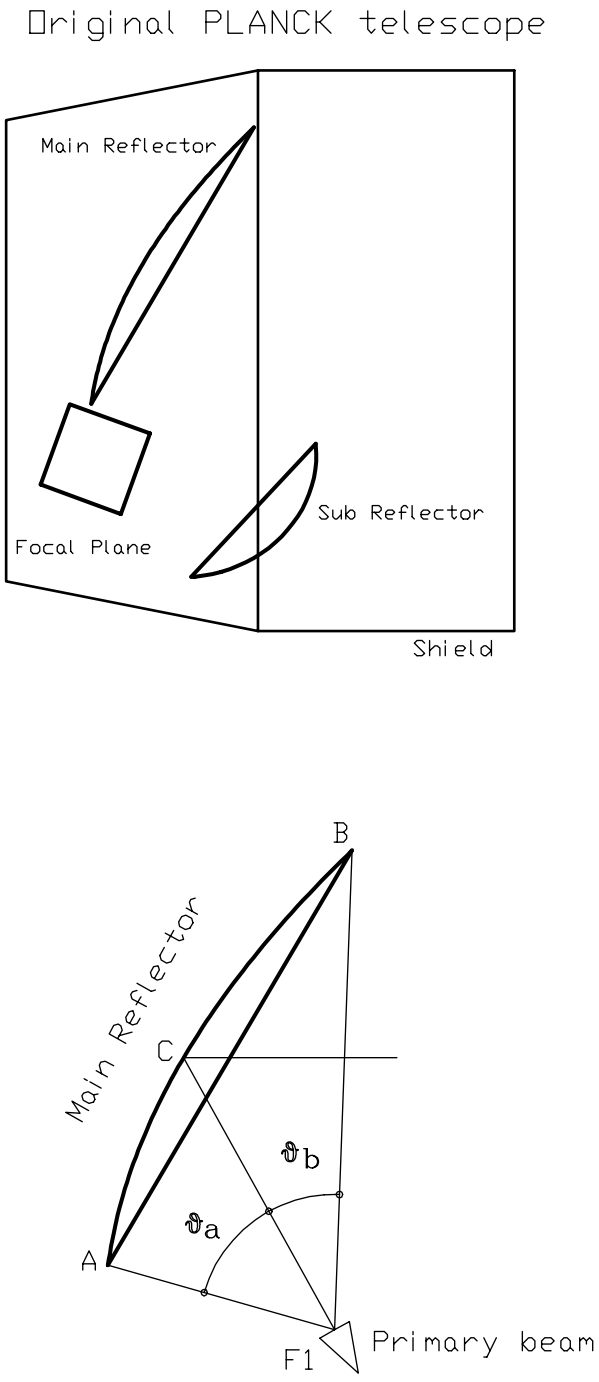

Figure 2: Upper table: original telescope design; Bottom table: parameters of main reflector far field simulations (see section 4).

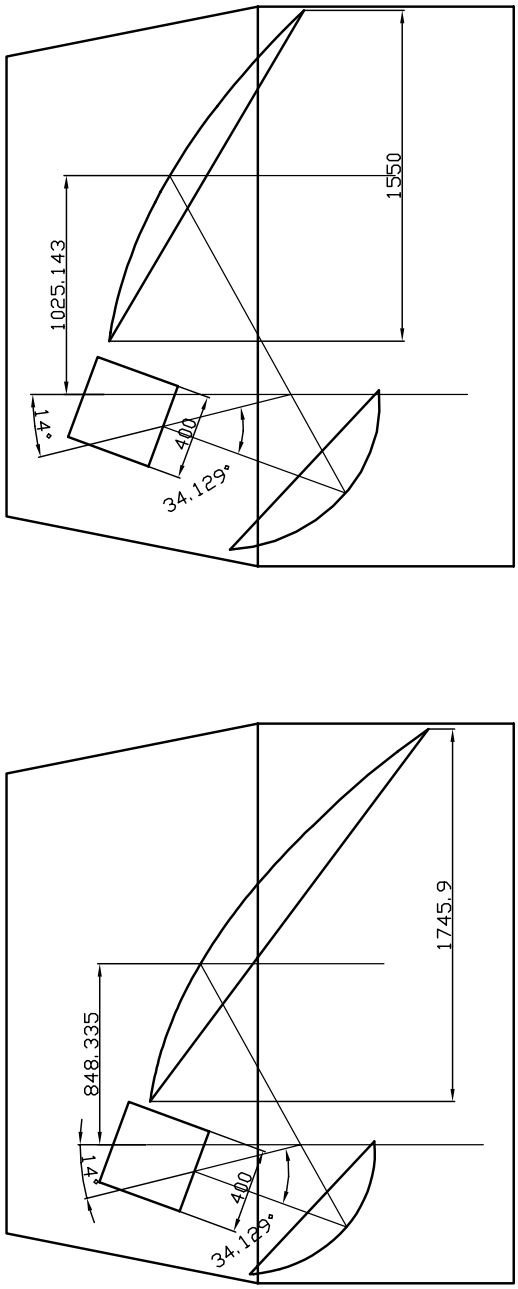

Figure 3: Design of the Conf.#1 - upper table - and of the Conf.#2 - bottom table.

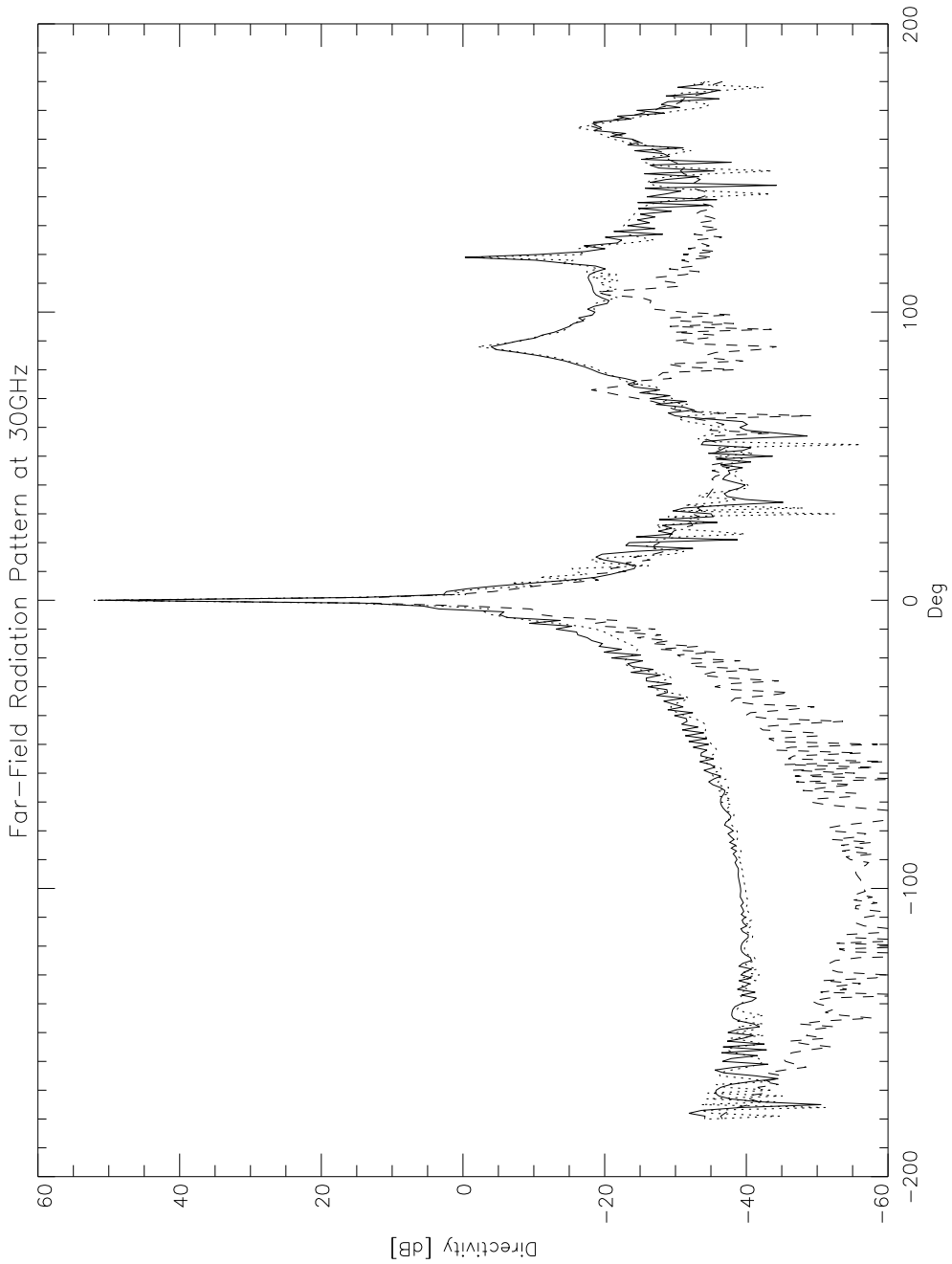

Figure 4: Far Field analysis results for the Planck telescope at 30GHz - Symmetry Plane. Conf.#0: solid line; Conf.#1: dotted line; Conf.#2: dashed line. The feed is pointed along the $\theta_a \neq \theta_b$ direction.

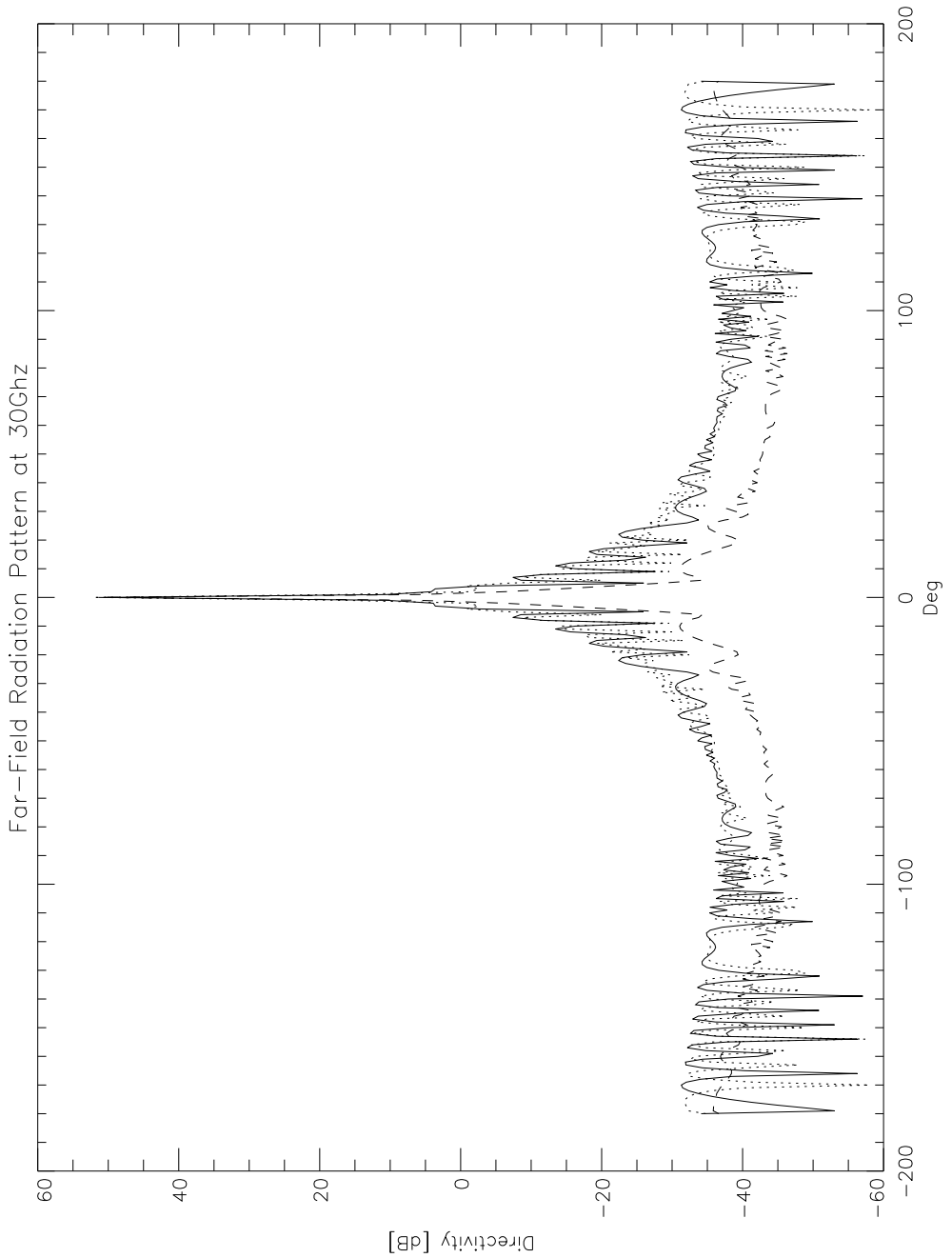

Figure 5: Far Field analysis results for the Planck telescope at 30GHz - Asymmetry Plane. Conf.#0: solid line; Conf.#1: dotted line; Conf.#2: dashed line. The feed is pointed along the $\theta_a \neq \theta_b$ direction.

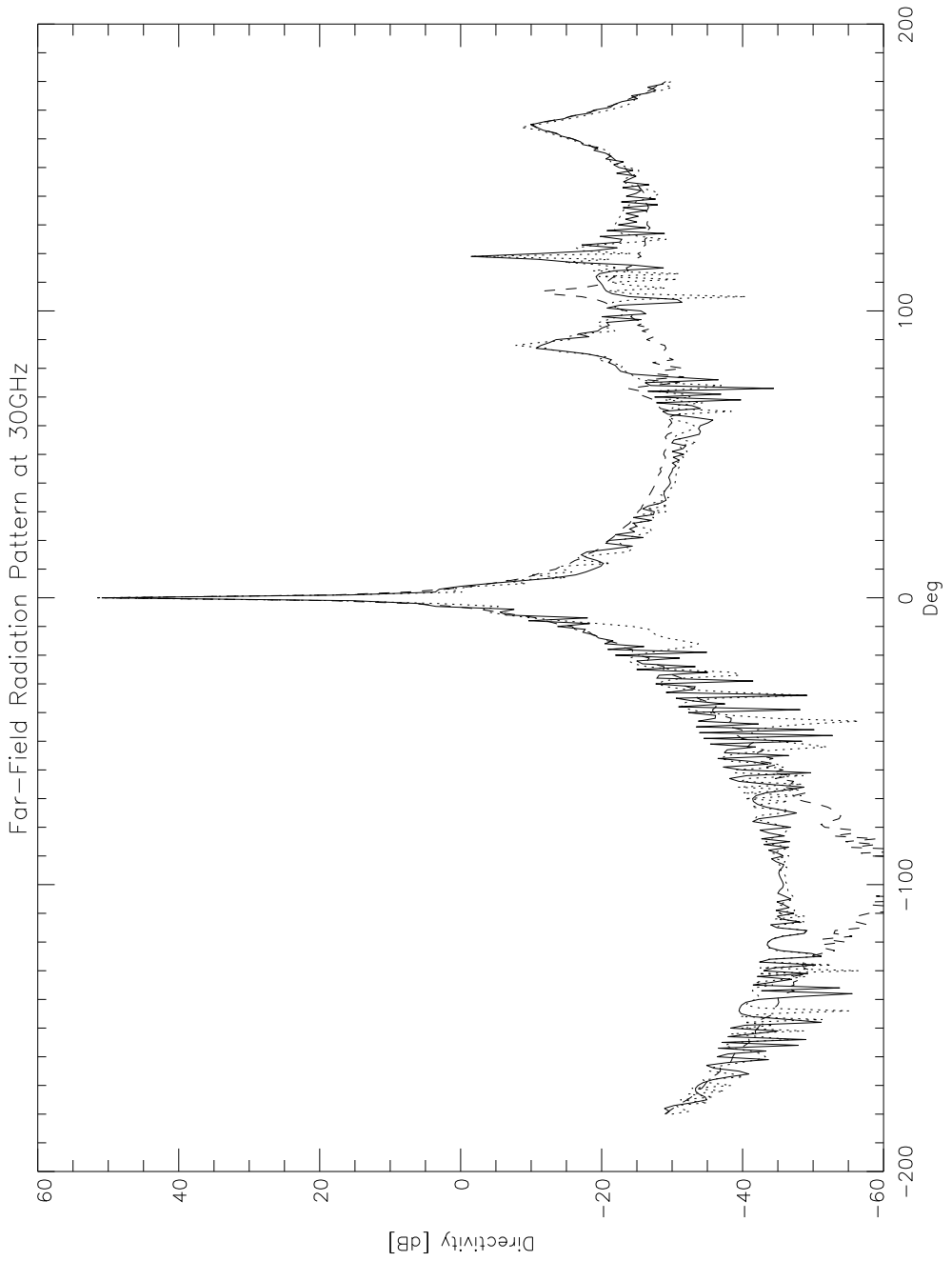

Figure 6: Far Field analysis results for the Planck telescope at 30GHz - Symmetry Plane. Conf.#0: solid line; Conf.#1: dotted line; Conf.#2: dashed line. The feed is pointed along the e $\theta_a = \theta_b$ direction.

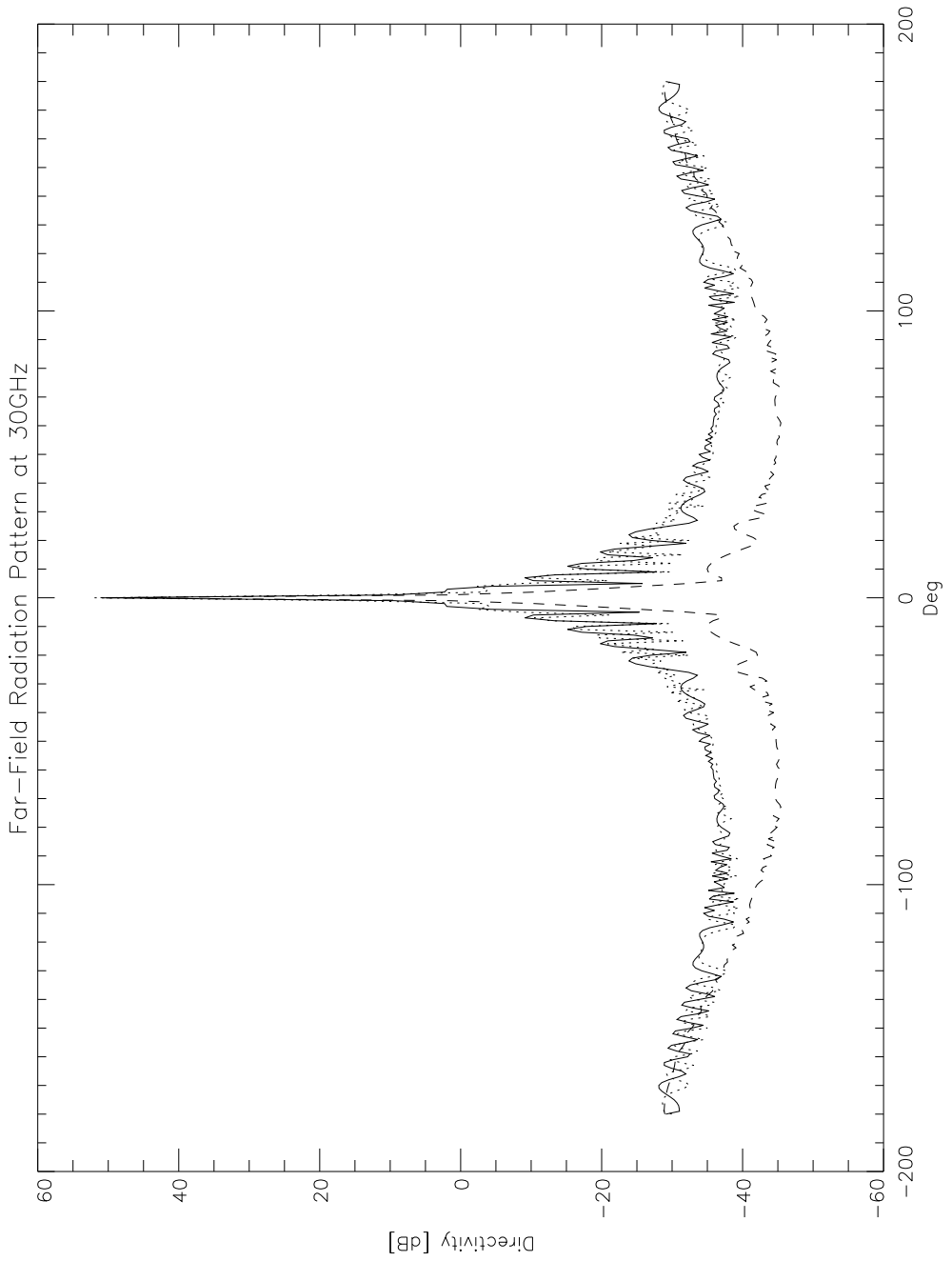

Figure 7: Far Field analysis results for the Planck telescope at 30GHz - Asymmetry Plane. Conf.#0: solid line; Conf.#1: dotted line; Conf.#2: dashed line. The feed is pointed along the e $\theta_a = \theta_b$ direction.

	Conf.#0	**Conf.#1**	**Conf.#2**
		Main Reflector	
D_p	1292.4	1550	1745.9
F_p	720	870	720
A	$(202.135, 14.187)$	$(250.143, 17.980)$	$(202.135, 14.187)$
B	$(1494.535, 775.568)$	$(1800.143, 931.182)$	$(1948.035, 1317.653)$
C	$(848.335, 249.886)$	$(1025.143, 301.988)$	$(848.335, 249.886)$
C_a	$(848.335, 249.886)$	$(1025.143, 301.988)$	$(1075.070, 401.311)$
2γ	61.01^o	61.01^o	61.01^o
		Sub Reflector	
M	2.5	2.5	2.5
$2a$	1200	1440	1200
$2c$	514.29	617.142	514.29
2β	14^o	14^o	14^o
2α	34.129^o	34.129^o	34.129^o
F_{eq}	1800	2175	1800
$F_{\#eq}$	1.39	1.40	$\sim$1.4

Table 1: *Parameters of Conf.#0 and of two new configurations of PLANCK telescope.* D_p *is the projected aperture diameter in a plane normal to the line of sight,* F_p *is the focal length of main reflector,* M *is the subreflector magnitude defined by* $M = |\frac{e+1}{e-1}|$*, where* e *is the eccentricity of ellipsoid of revolution,* $2a$ *is the major axis of subreflector,* $2c$ *is the focal length of subreflector,* 2β *is the offset angle between paraboloid axis of revolution and ellipsoid axis of revolution,* F_{eq} *is the equivalent focal length and* $F_{\#eq}$ *is the equivalent focal ratio. For the definition of the angles* 2α *and* 2γ *see the figure 1. Linear measurements are in mm and angles in degree. As we can see in this table, the center of the aperture coincides with the intersection between the central ray and the main reflector profile only for the Conf.#0 and the Conf.#1.*

30GHz	Dir (dB)	HPBW (')
Conf.#0	50.4	34'
Conf.#1	52.0	28'
Conf.#2	51.2	30'

Table 2: *Directivity (Dir) and Half Power Beam Width (HPBW) at 30GHz.*

100GHz	Dir (dB)	HPBW (')
Conf.#0	60.7	10'
Conf.#1	62.4	8'
Conf.#2	61.4	9'

Table 3: *Directivity (Dir) and Half Power Beam Width (HPBW) at 100GHz.*